

UC San Diego

UC San Diego Previously Published Works

Title

Nuclear miR-320 Mediates Diabetes-Induced Cardiac Dysfunction by Activating Transcription of Fatty Acid Metabolic Genes to Cause Lipotoxicity in the Heart

Permalink

<https://escholarship.org/uc/item/7m89k316>

Journal

Circulation Research, 125(12)

ISSN

0009-7330

Authors

Li, Huaping
Fan, Jiahui
Zhao, Yanru
et al.

Publication Date

2019-12-06

DOI

10.1161/circresaha.119.314898

Peer reviewed



Nuclear miR-320 Mediates Diabetes-Induced Cardiac Dysfunction by Activating Transcription of Fatty Acid Metabolic Genes to Cause Lipotoxicity in the Heart

Huaping Li,* Jiahui Fan,* Yanru Zhao,* Xiaorong Zhang, Beibei Dai, Jiabing Zhan, Zhongwei Yin, Xiang Nie, Xiang-Dong Fu, Chen Chen, Dao Wen Wang

RATIONALE: Diabetes mellitus is often associated with cardiovascular complications, which is the leading cause of morbidity and mortality among patients with diabetes mellitus, but little is known about the mechanism that connects diabetes mellitus to the development of cardiovascular dysfunction.

OBJECTIVE: We aim to elucidate the mechanism underlying hyperglycemia-induced cardiac dysfunction on a well-established db/db mouse model for diabetes mellitus and diabetic complications that lead to heart failure.

METHODS AND RESULTS: We first profiled the expression of microRNAs (miRNAs) by microarray and quantitative reverse transcription polymerase chain reaction on db/db mice and identified miR-320 as a key miRNA associated with the disease phenotype. We next established the clinical relevance of this finding by showing the upregulation of the same miRNA in the failing heart of patients with diabetes mellitus. We demonstrated the causal role of miR-320 in inducing diabetic cardiomyopathy, showing that miR-320 overexpression exacerbated while its inhibition improved the cardiac phenotype in db/db mice. Unexpectedly, we found that miR-320 acts as a small activating RNA in the nucleus at the level of transcription. By chromatin immunoprecipitation sequencing and chromatin immunoprecipitation quantitative polymerase chain reaction analysis of Ago2 (argonaute RISC catalytic component 2) and RNA polymerase II in response to miR-320 induction, we identified *CD36* (fatty acid translocase) as a key target gene for this miRNA and showed that the induced expression of *CD36* is responsible for increased fatty acid uptake, thereby causing lipotoxicity in the heart.

CONCLUSIONS: These findings uncover a novel mechanism for diabetes mellitus-triggered cardiac dysfunction, provide an endogenous case for small activating RNA that has been demonstrated to date only with synthetic RNAs in transfected cells, and suggest a potential strategy to develop a miRNA-based therapy to treat diabetes mellitus-associated cardiovascular complications.

VISUAL OVERVIEW: An online [visual overview](#) is available for this article.

Key Words: CD36 antigens ■ cell nucleus ■ diabetic cardiomyopathies ■ fatty acids ■ microRNAs

Editorial, see p 1121 | Meet the First Author, see p 1036

Correspondence to: Chen Chen, MD, PhD, Division of Cardiology, Department of Internal Medicine, Tongji Hospital, Tongji Medical College, Huazhong University of Science and Technology, 1095 Jiefang Ave, Wuhan 430030, China, Email chenchen@tjh.tjmu.edu.cn; or Dao Wen Wang, MD, PhD, Division of Cardiology, Department of Internal Medicine, Tongji Hospital, Tongji Medical College, Huazhong University of Science and Technology, 1095 Jiefang Ave, Wuhan 430030, China, Email dwwang@tjh.tjmu.edu.cn

*H.L., J.F., and Y.Z. contributed equally to this article.

The online-only Data Supplement is available with this article at <https://www.ahajournals.org/doi/suppl/10.1161/CIRCRESAHA.119.314898>.

For Sources of Funding and Disclosures, see page 1119.

© 2019 The Authors. *Circulation Research* is published on behalf of the American Heart Association, Inc., by Wolters Kluwer Health, Inc. This is an open access article under the terms of the [Creative Commons Attribution Non-Commercial-NoDerivs](#) License, which permits use, distribution, and reproduction in any medium, provided that the original work is properly cited, the use is noncommercial, and no modifications or adaptations are made.

Circulation Research is available at www.ahajournals.org/journal/res

Novelty and Significance

What Is Known?

- Intensive glycemic control has been found to be insufficient in reducing the risk of heart failure among diabetic patients.
- Glycemic control does not rescue hyperglycemia-induced microRNA (miRNA) expression in diabetic hearts.
- miRNAs typically suppress gene expression at the post-transcriptional level in the cytoplasm, but increasing evidence also suggests a role for miRNAs in the nucleus.

What New Information Does This Article Contribute?

- MiR-320 is significantly upregulated in the diabetic myocardium in mice and patients and translocates into the nucleus to directly enhance *CD36* (fatty acid translocase) transcription.
- MiR-320/*CD36* pathway links glucose toxicity to lipotoxicity in the heart, which provides new diabetic cardiomyopathy insights.
- Recombinant adeno-associated virus (type 9)-mediated miR-320 tough decoy (inhibitor) delivery rescues cardiac dysfunction in db/db mice.

Diabetes mellitus is often associated with cardiovascular complications, which is the leading cause of morbidity and mortality among patients with diabetes mellitus, but little is known about the mechanism that connects diabetes mellitus to the development of cardiovascular dysfunction. Herein, we identified miR-320 as a key miRNA associated with the disease phenotype. We demonstrated the causal role of miR-320 in inducing diabetic cardiomyopathy, showing that miR-320 overexpression exacerbated while its inhibition improved the cardiac phenotype in db/db mice. Unexpectedly, we found that miR-320 acts as a small activating RNA in the nucleus at the level of transcription. Moreover, we identified *CD36* as a key target gene for this miRNA and showed that the induced expression of *CD36* is responsible for increased fatty acid uptake, thereby causing lipotoxicity in the heart. These findings uncover a novel mechanism for diabetic-triggered cardiac dysfunction and suggest a potential strategy to develop a miRNA-based therapy to treat diabetes mellitus-associated cardiovascular complications.

Nonstandard Abbreviations and Acronyms

DCM	diabetic cardiomyopathy
FA	fatty acid
FAO	fatty acid oxidation
FFA	free fatty acid
HFD	high-fat diet
miRNA	microRNA
NRVC	neonatal rat ventricular cardiomyocyte
rAAV	recombinant adeno-associated virus
RISC	RNA-induced silencing complex
SGLT2	sodium-glucose cotransporter 2
tg	transgenic
tnt	troponin T
TuD	tough decoy
VLDLR	very-low-density lipoprotein receptor
wt	wild type

increased fatty acid (FA) utilization, lipotoxicity, elevated apoptotic and necrotic cell death, impaired Ca^{2+} balance, mitochondrial dysfunction, altered myocardial insulin signaling, and oxidative and endoplasmic reticulum stress.² However, it has been virtually unclear about the causal relationships among these complications.

Despite the fact that diabetic conditions are linked to the development of cardiac dysfunction and prognosis is worse for heart failure patients with abnormal levels of glycated hemoglobin, intensive glycemic control has been found to be insufficient in reducing the risk of heart failure among patients with diabetes mellitus,³ implying that diabetes mellitus-associated cardiac dysfunction may be induced by other metabolic triggers. In fact, diabetes mellitus has been characterized by hyperlipidemia and hyperinsulinemia, both of which are known to precede pancreatic cell failure.⁴ Resulting hyperglycemia can further enhance FA uptake and myocardial steatosis,⁵ which may lead a vicious cycle between elevated glucose toxicity and lipotoxicity to drive the development of heart failure. In terms of the treatment, although recent studies have demonstrated that SGLT2 (sodium-glucose cotransporter 2) inhibitor canagliflozin—a new drug for diabetes mellitus—reduced the risk of cardiovascular death or hospitalized heart failure in patients with type 2 diabetes mellitus and an elevated risk of cardiovascular disease, the exact mechanisms and whether it functions on DCM are still not defined.^{3,6}

By 2025, the number of individuals with diabetes mellitus worldwide is predicted to be ≈300 million. Cardiovascular disease accounts for 80% of death among diabetic patients, which often leads to heart failure.¹ Diabetic cardiomyopathy (DCM) is characterized by changes in myocardial structure and function, which is known to associate with a variety of complications, including advanced glycation end products, fibrosis,

microRNA (miRNA) is a class of small (≈ 22 nt) non-coding RNAs with well-established functions in cancer, metabolic disorders, and cardiovascular diseases. A recent study identified 316 miRNAs dysregulated in the heart of streptozotocin-induced diabetes mellitus mice, and importantly, glycemic control was found to be unable to rescue such hyperglycemia-induced miRNA expression in diabetic heart,⁷ suggesting a potential contribution of miRNAs to the development of diabetes mellitus-induced cardiac dysfunction. miRNAs typically suppress gene expression at posttranscriptional levels in the cytoplasm, but increasing evidence also suggests roles of miRNAs in the nucleus, as well as in the mitochondria.^{8,9} Despite their clear linkage to various diseases, it has remained largely elusive about how specific miRNAs might contribute to defined disease pathways.

In this study, we report the upregulation of the miRNA miR-320 in the failing heart of diabetes mellitus mice (db/db), as well as in patients with diabetes mellitus. Unexpectedly, we found that miR-320 is efficiently translocated to the nucleus where it enhances *CD36* (fatty acid translocase) transcription, leading to enhanced uptake of free FAs (FFA), thereby causing myocardial lipotoxicity. We demonstrated that an miR-320 tough decoy (TuD) delivered by recombinant adeno-associated virus (rAAV) is able to rescue the cardiac dysfunction in diabetes mellitus mice, suggesting a potential therapy for diabetes mellitus-associated cardiac dysfunction.

METHODS

An expanded version of the Methods, including detailed experimental procedures on animals, microarrays, high-throughput sequencing, a list of polymerase chain reaction primers, and antibodies, is presented in the [Online Data Supplement](#).

The raw sequencing and microarray data that support the findings of this study are available from the corresponding authors on request.

Ethics Statement

Human heart and plasma samples were collected at Tongji Hospital (Wuhan, China) between January 2012 and October 2014. The study, approved by the Ethics Review Board of Tongji Hospital and Tongji Medical College, conforms to the principles outlined in the Declaration of Helsinki. Written, informed consent was obtained from individual subjects or their immediate family members in cases of incapacitation. The animal study was performed in strict accordance with the recommendations of the Guide for the Care and Use of Laboratory Animals of the National Institutes of Health. The protocol was approved by the Committee on the Ethics of Animal Experiments of the Animal Research Committee of Tongji College.

Transcriptome Analysis and miRNA Profiling

miRNA and mRNA sequencing and data analysis were performed by Personal Biotechnology Co (Shanghai, China). Microarray analysis on human heart miRNAs was performed by Kangcheng

Bio-tech (Shanghai, China) using the Exiqon miRCURY LNA miRNA Arrays (seventh generation). Microarray analysis of heart samples from db/db and wt (wild type) mice was performed at CapitalBio (Beijing, China) on GeneChip Mouse Genome 430 2.0 Arrays from Affymetrix (Santa Clara, CA). The methods and partial results were described in our previous work.¹⁰

Generation of miR-320 tg Mice and In Situ Hybridization

To generate miR-320 tg (transgenic) mice, a DNA fragment containing murine miR-320 was inserted into the pUBC vector for expression under the control of the ubiquitin C promoter. Microinjection was performed according to standard protocols. miR-320 tg mice were backcrossed into the C57BL/6 background for 6 generations, yielding wt and miR-320 tg mice that were $>95\%$ of the C57BL/6 genotype. The primers for genotyping miR-320 tg mice were 5'-CCACTGCTTACTGGCTTATCG-3' (forward) and R 5'-ATGAAGCACCTCCG

CTGAG-3' (reverse). miRNA in situ hybridization was performed on formalin-fixed and paraffin-embedded tissue specimens as described previously.¹¹

Prediction of miRNA Targets

The RNAhybrid (<https://bibiserv.cebitec.uni-bielefeld.de/rna-hybrid/submission.html>) and miRBase (<http://www.mirbase.org/>) websites were used for miR-320 target prediction. Base-pairing at least 7 consecutive nucleotides (allowing G:U wobbles) and a minimum free energy of hybridization lower than -20 kcal/mol, which have been shown to be sufficient for formation of a miRNA/mRNA complex,¹² were used as a cutoff to identify potential miRNA targets.

rAAV Administration

Male wt and db/db mice (from the Model Animal Research Center of Nanjing University, China) were divided into rAAV9 treatment (rAAV-miR-random, rAAV-miR-320, rAAV-miR-320 TuD (inhibitor) and rAAV9-tnt-treatment (rAAV-tnt-miR-random, rAAV-tnt-miR-320, and rAAV-tnt-miR-320 TuD, rAAV-tnt-CD36, rAAV-tnt-CD36-shRNA) groups. The detailed experimental procedure on animals is presented in the [Online Data Supplement](#).

Statistical Analysis

Tests for statistical significance were computed using the Prism, version 8.0.2, software (GraphPad Software, San Diego, CA) with a probability value of <0.05 considered significant. Each data set, irrespective of the sample size, was tested for normality typically using the Shapiro-Wilk test. Thereafter, a parametric or nonparametric test was chosen as appropriate. Statistical analyses were then performed with 2-tailed Student *t* test (parametric unpaired or paired, 2 group of analysis), Wilcoxon signed-rank test (nonparametric paired, 2 group of analysis), Mann-Whitney *U* test (nonparametric unpaired, 2 group of analysis), 1-way ANOVA combined with Bonferroni multiple comparisons (comparisons between >2 groups, parametric unpaired), and Kruskal-Wallis ANOVA test with Dunn multiple comparisons test (comparisons between >2 groups, nonparametric unpaired). Two-way ANOVA followed by Dunnett post hoc test was used in the in vivo studies on the same continuous mice when multiple time points were

involved. Data are represented as mean \pm SEM, unless otherwise stated. A value of *P* (or corrected *P* in case of multiple groups) <0.05 was considered to be statistically significant.

RESULTS

miR-320 Is Upregulated in Cardiomyocytes Under Diabetic Conditions

The leptin receptor-deficient db/db mouse is a well-established rodent model for type 2 diabetes mellitus and diabetic complications.¹³ Cardiac function is clearly compromised at the age of 6 months in these mice.¹⁴ To identify dysregulated miRNAs in this diabetes mellitus-induced cardiac dysfunction model, we performed small RNA sequencing on hearts from 6-month-old db/db mice in comparison with wt mice. A total of 1024 miRNAs were detected in the heart, of which 256 with the transcript per kilobase million value of >1 were selected for further analysis. This led to the identification of 21 miRNAs that were significantly dysregulated in the heart of db/db mice as compared with wt controls (Figure 1A).

We previously profiled miRNAs in patients with heart failure by microarray.¹⁵ Intersection of the current results from db/db mice with the patient data revealed that, among 21 dysregulated miRNAs, miR-340-5p, miR-34a-5p, and miR-320 were upregulated in the failing heart of patients with diabetes mellitus but not in the nondiabetic patients (Online Figure 1A; Online Table I). As miR-320 was more abundant than miR-340-5p and miR-34a-5p in human heart (Online Figure 1B), we decided to focus on this miRNA for detailed mechanistic study.

By quantitative reverse transcription PCR (RT-qPCR), we found that the levels of circulating and cardiac miR-320 were increased in heart failure patients with diabetes mellitus (Online Figure 1C; Online Tables II and III), as well as in db/db mice (Figure 1B). We further demonstrated that this miRNA was specifically elevated in cardiomyocytes (Figure 1C; Online Figure 1D). We also made similar observations in a high-fat diet (HFD)-induced cardiac dysfunction model (Online Figure 1E and 1F). We further observed that elevated blood glucose preceded the increase in cardiac miR-320 expression ahead of observable cardiac systolic dysfunction (Figure 1D through 1F; Online Figure 1G through 1I; Online Table IV). A similar regulation pattern was also observed in db/db mice model at multiple time points (Online Figure 1J through 1O; Online Table V). These temporal events in both mice and humans suggest a potential causal role of high glucose-induced expression of miR-320 to the initiation of diabetes mellitus-induced cardiac dysfunction.

Diabetes Mellitus-Induced Cardiac Dysfunction Is Exacerbated by miR-320 Overexpression and Rescued by miR-320 Inhibition

To demonstrate the causal role of miR-320 in diabetes mellitus-induced cardiac dysfunction, we used

miR-320-overexpressing tg mice to evaluate miR-320 function in HFD-induced cardiac dysfunction model (Online Figure 1IA). As expected, miR-320 was highly expressed in the heart of these tg mice (Online Figure 1IB and 1IC), and HFD exacerbated cardiac dysfunction (Figure 2A; Online Table VI), which was accompanied with increased myocardium size (Figure 2B) and apoptosis (Figure 2C; Online Figure 1ID) relative to wt mice. In contrast, cardiac function was similar between miR-320 tg and wt mice when fed with normal diet (Figure 2A), indicating that overexpressed miR-320 exerts adverse effects on the heart selectively under diabetic conditions.

We further characterized the miR-320 tg mice, showing a greater increase in body weight, glucose levels, and insulin resistance than their wt counterparts when fed with HFD (Online Figure 1IE and 1IF). To clarify the specific role of miR-320 in the heart, we used an rAAV9 system (with cardiac specificity at 1×10^{11} vector copy numbers)¹⁶ to express miR-320 or an miR-320 inhibitor based on the TuD design in db/db mice for long-term (16 weeks) effects. Real-time polymerase chain reaction confirmed that rAAV delivery increased the miR-320 level in the heart (Online Figure 1IG and 1IH). Blood glucose level and body weight did not differ among mice 4 months after rAAV delivery (Online Figure 1II); however, cardiac dysfunction was exacerbated by miR-320 overexpression but relieved upon miR-320 inhibition (Figure 2D; Online Table VII). Hematoxylin and eosin staining of myocardial tissue sections and terminal deoxynucleotidyl transferase dUTP nick end labeling indicated that rAAV-miR-320 treatment increased cardiac myocyte size and apoptosis in db/db mice (Figure 2E and 2F), whereas rAAV-miR-320-TuD showed the opposite effects. We additionally explored potential short-term (8 weeks) effects of rAAV-miR-320 treatment on cardiac function. Notably, compared with long-term interventions, the echocardiographic and hemodynamic data from relatively short-term treatment showed similar trends in db/db mice (Online Figure 1IJ through 1IM; Online Table VIII), confirming the consistent and persistent effects of miR-320 in inducing DCM. Importantly, we never saw significant differences on wt mice, indicating the effect of miR-320 on the heart only under diabetic conditions (Online Figure 1IJ through 1IM; Online Table VIII). Interestingly, besides db/db and HFD-induced diabetic models, miR-320 also showed similar regulation on cardiac function in another diabetic model induced by streptozotocin (Online Figure 1IN through 1IP). Collectively, these results strongly suggest that miR-320 is directly involved in diabetes mellitus-induced cardiac dysfunction.

miR-320 Acts in the Nucleus

Pre-miRNAs undergo a series of biogenesis steps to generate mature miRNAs, which typically function to regulate gene expression at posttranscription levels in the cytoplasm. As part of our efforts in systematically characterizing biogenesis and function of miR-320 under

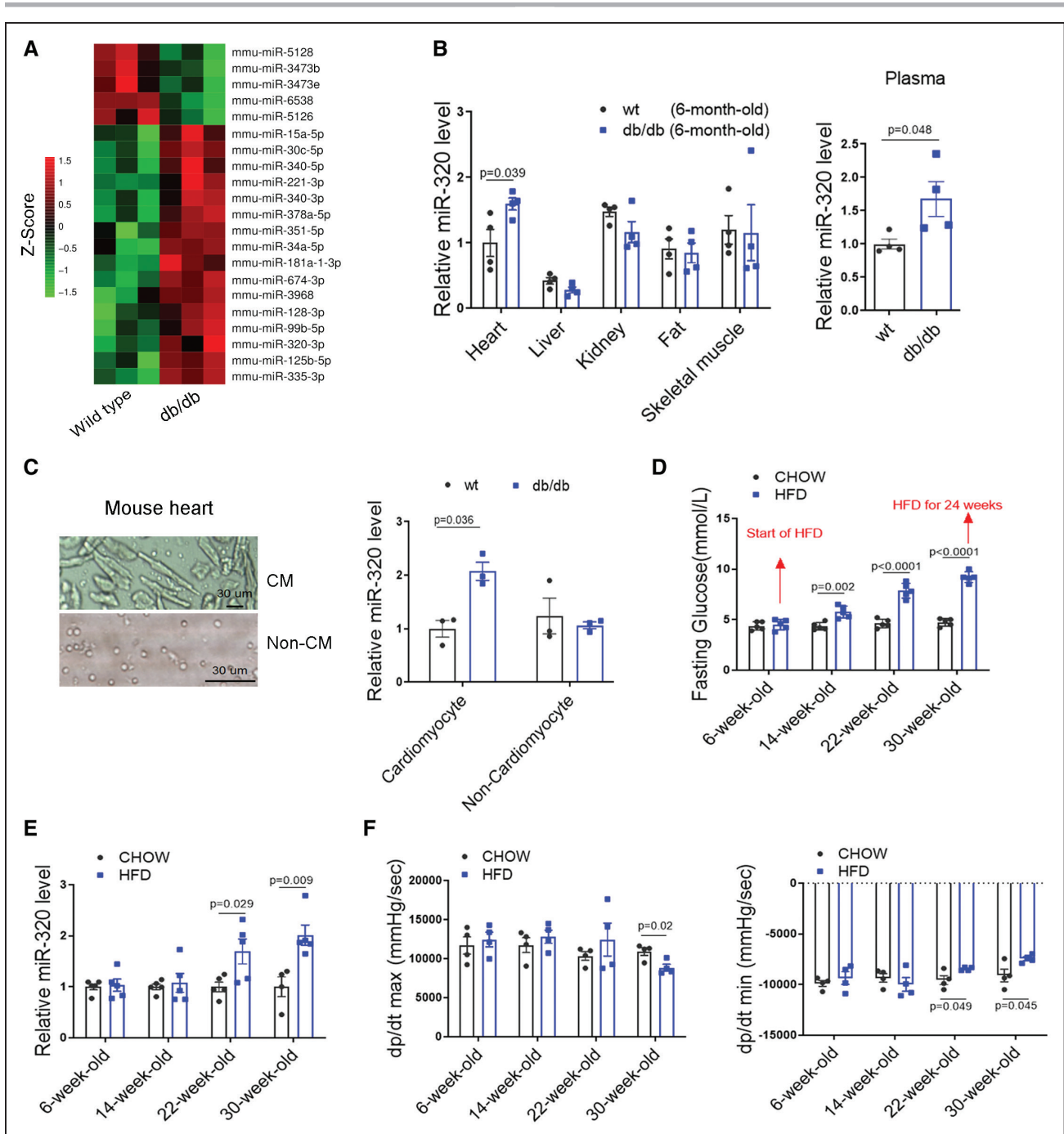


Figure 1. miR-320 is upregulated in cardiomyocytes of diabetic mice.

A, Z score transformed heat map of microRNA sequencing results on 6-mo-old db/db in comparison with wt (wild type) mice ($n=3$; fold change, >1.5 ; $P<0.05$). **B** and **C**, Quantitative reverse transcription polymerase chain reaction analysis of miR-320 expression in various tissues (**B**) and cardiomyocytes (CMs) and noncardiomyocytes (NCMs) in db/db mice. miR-320 levels in other tissues of db/db diabetic mice are represented as fold change relative to the heart. miR-320 level in NCMs was presented as fold change relative to CMs. **D–F**, Time-course analysis of fasting glucose (**D**), cardiac miR-320 level (**E**), and cardiac function (**F**) in high-fat diet (HFD)-induced diabetic mice. **A**, $n=3$; (**B** and **C**) $n=3$ to 4; (**D–F**) $n=4$ to 6. **B**, Student *t* test; (**C**) 1-way ANOVA followed by Bonferroni post test (number of comparisons, 6); (**D–F**) Student *t* test. Adjusted *P* values were provided in case of multiple groups.

physiological and pathological conditions, we examined the subcellular localization of miR-320 in diabetic and normal hearts by in situ hybridization. Surprisingly, we noted that miR-320 was present in the nucleus of mouse myocytes (Figure 3A through 3C). This was further

confirmed with stem-loop polymerase chain reaction, which specifically detects the mature form of miRNAs, on both cytosolic and nuclear fractions (Online Figure IIIA). Compared with wt heart, the level of miR-320 was further increased in the nucleus but remained largely unchanged

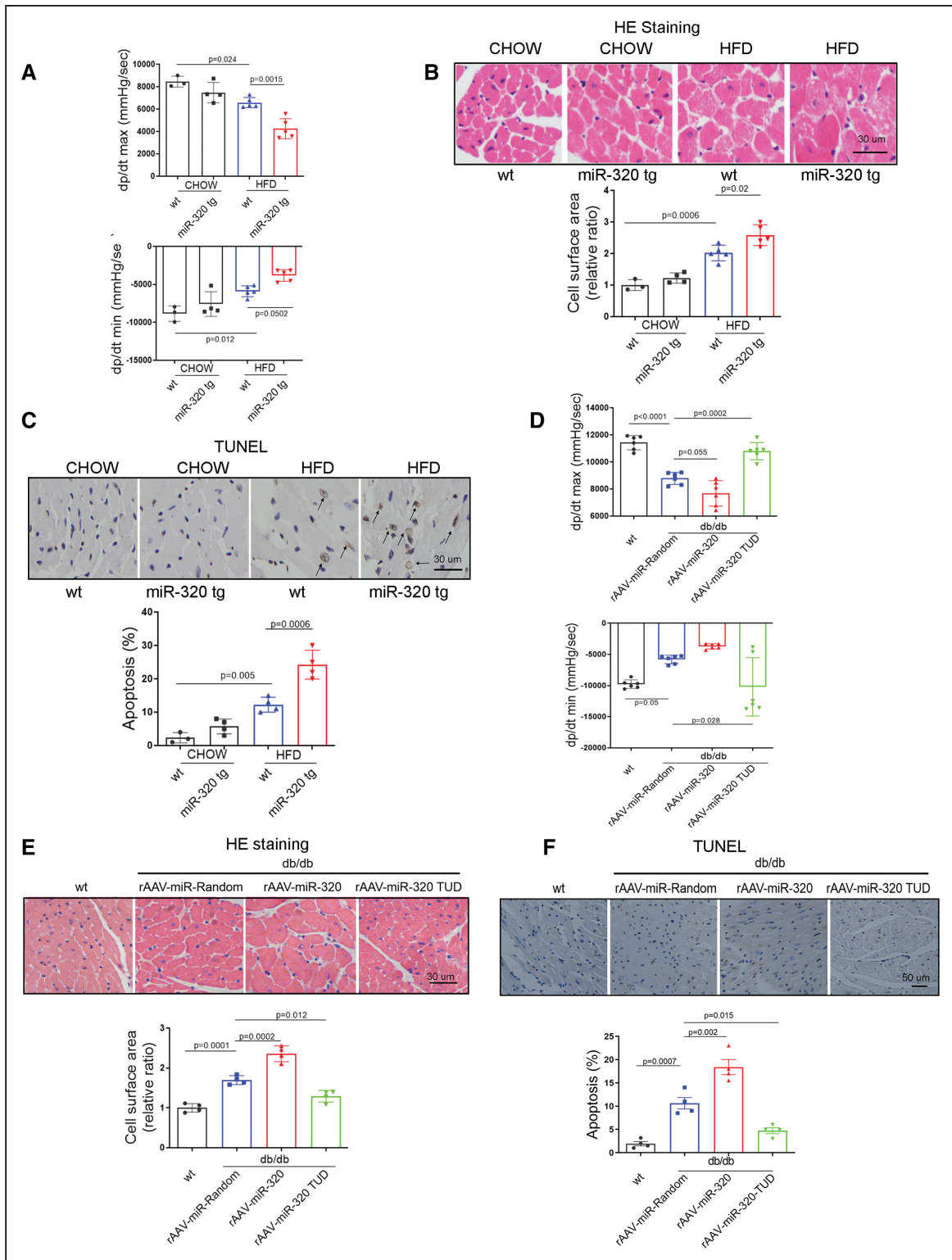


Figure 2. Cardiac dysfunction in diabetes mellitus is exacerbated by miR-320 and rescued by miR-320 inhibition.

A, Hemodynamic analysis of miR-320 tg (transgenic) and wt (wild type) mice under normal diet and high-fat diet (HFD) for 6 mo. dp/dt max and dp/dt min, peak instantaneous rate of left ventricular pressure increase and decrease, respectively. wt-CHOW, n=3; miR-320 tg-CHOW, n=4; wt-HFD, n=5; miR-320 tg-HFD, n=5. **B**, Cardiomyocyte (CM) visualization and size quantitation on miR-320 tg and wt mice. **C**, Visualization of cardiac apoptosis by terminal deoxynucleotidyl transferase dUTP nick end labeling (TUNEL) on miR-320 tg and wt mice. **D–F**, Hemodynamic analysis (**D**), hematoxylin and eosin (HE) staining (**E**), and TUNEL (**F**) of myocardial tissues in db/db mice with various treatments. **A–C**, n=3 to 5; (**D**) n=6; (**E** and **F**) n=4; (**A–F**) 1-way ANOVA followed by Bonferroni post test (number of comparisons, 6). Adjusted *P* values were provided in case of multiple groups. rAAV indicates recombinant adeno-associated virus.

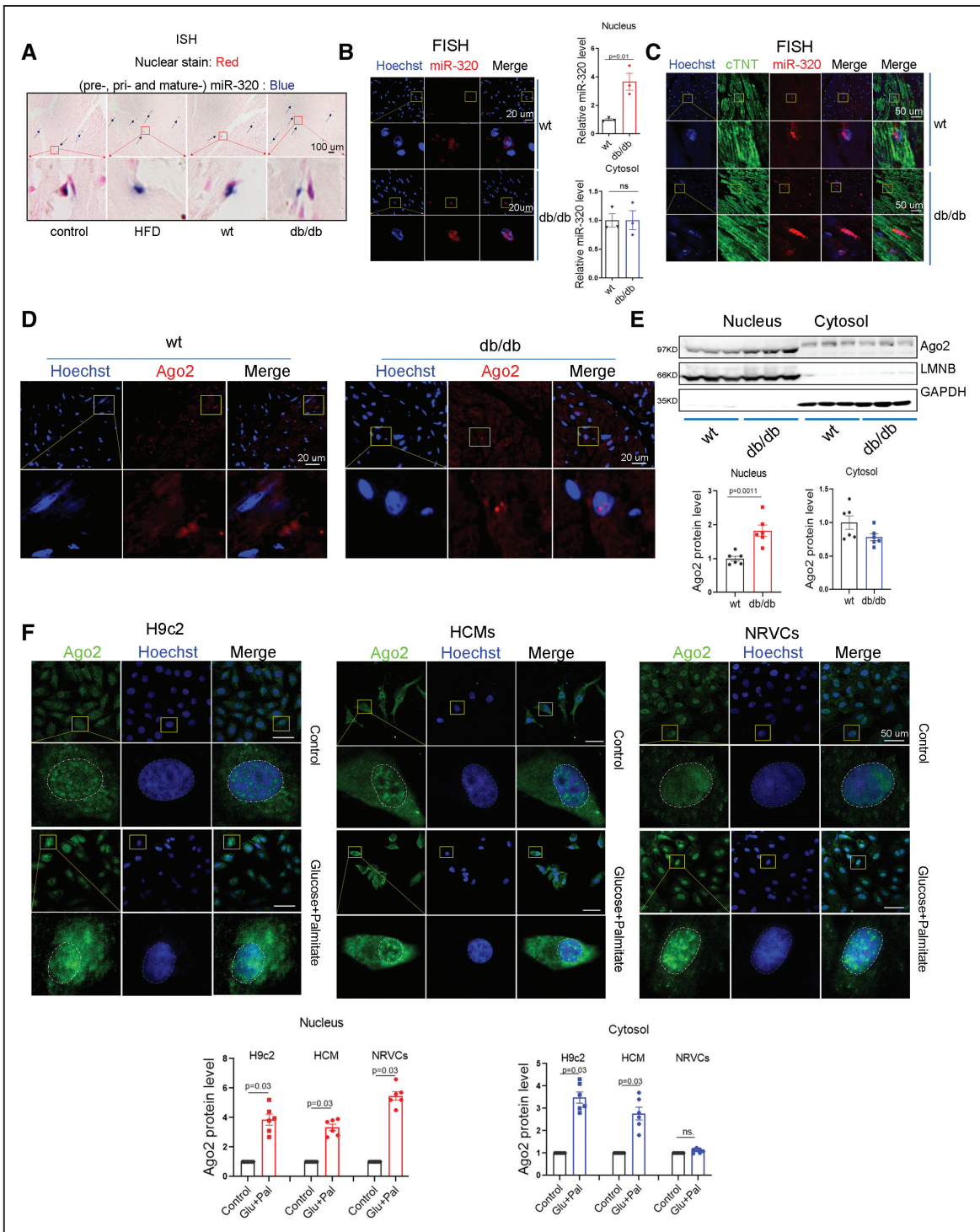


Figure 3. Nuclear localization of miR-320 and Ago2 (argonaute RISC catalytic component 2).

A and **B**, Nuclear localization of miR-320 in heart sections, as detected by in situ hybridization (**A**) and fluorescence in situ hybridization (FISH; **B**). **C**, Colocalization of miR-320 with the myocyte marker cTNT (cardiac muscle troponin T) in heart sections by fluorescent in situ hybridization. **D**, Immunofluorescence detection of Ago2 and Hoechst in db/db mice heart. **E**, Immunoblotting detection of Ago2, LMNB (lamin B), and GAPDH (glyceraldehyde-3-phosphate dehydrogenase) in nuclear and cytoplasmic fractions from db/db mice heart. **F**, Immunofluorescence detection of Ago2 and Hoechst in H9c2, human primary cardiomyocytes (HCMs), and neonatal rat ventricular cardiomyocytes (NRVCs) cultured with high glucose (33.3 mmol/L) and palmitate (0.5 mmol/L) for 24 h. **A–D**, $n=3$; (**E** and **F**) $n=6$; **B** and **E**, Student *t* test; (**F**) Wilcoxon signed-rank test. ISH indicates in situ hybridization.

in the cytosol of db/db mice (Online Figure IIIB). Moreover, cardiomyocytes with elevated levels of nuclear miR-320 also showed terminal deoxynucleotidyl transferase

dUTP nick end labeling signals (Online Figure IIIC and IIID), supporting a potential causal role of miR-320 in diabetes mellitus-induced myocyte apoptosis. In sharp

contrast, miR-320 was neither colocalized with fibroblast- nor endothelial-specific markers in diabetic heart (Online Figure IIIE). We further determined the localization of miR-320 in cultured H9c2 cell lines and neonatal rat ventricular cardiomyocytes (NRVCs), again confirming its nuclear distribution and miR-320 inhibitor treatment significantly decreased the fluorescence intensity of miR-320 fluorescence in situ hybridization signal (Online Figure IIIF and IIIG). Interestingly, miR-320 was specifically localized in nucleus of NRVCs (cardiomyocytes) but not noncardiomyocytes (Online Figure IIIH and IIIL). These findings suggest that miR-320 might have a selective role in the nucleus of cardiomyocytes, which is in line with increasing evidence for nuclear function of miRNAs. To obtain global evidence for this regulatory paradigm, we performed small RNA sequencing on fractionated cardiomyocytes, finding that miR-320 was more abundant in the nucleus than in the cytoplasm (Online Figure IIJJ). Notably, a subset of other miRNAs also showed similar nuclear enrichment (Online Figure IIJK through IIJM).

If miR-320 was induced in the nucleus of cardiomyocytes from db/db mice, we wondered whether Ago2 (argonaute RISC catalytic component 2)—a key component of the RISC (RNA-induced silencing complex)—also showed a detectable increase in the nucleus. Indeed, immunofluorescence and biochemical fractionation experiments revealed the nuclear accumulation of Ago2 in the heart of db/db mice as compared with wt control (Figure 3D and 3E; Online Figure IV). We further confirmed the elevated distribution of Ago2 in the nucleus of H9c2 cell lines, human primary cardiomyocytes, and NRVCs when cultured in the presence of high glucose and palmitate (Figure 3F). These findings point to a critical role of nuclear miR-320 in cardiomyocytes under diabetes mellitus conditions.

miR-320 Functions in Diabetes Mellitus-Induced Cardiac Dysfunction Through Induced CD36

Ago2 has been reported to preferentially associate with active promoters,⁹ suggesting a direct role of RISC in transcriptional control. We, therefore, investigated whether the Ago2-miR-320 complex might interact with specific gene promoters by searching for genes induced by nuclear miR-320 accompanied with diabetes mellitus-induced cardiac dysfunction (Figure 4A). We reasoned that candidate genes would (1) be dysregulated in diabetes mellitus-induced cardiac dysfunction, (2) show favorable sequence motifs for miR-320 binding near their promoter regions, and (3) respond to miR-320 induction. Using these criteria, we identified potential miR-320 target genes that might be directly responsible for diabetes mellitus-induced cardiac dysfunction.

We first performed mRNA microarray analysis of heart tissues from wt and db/db mice, identifying ≈600

differentially expressed genes (fold change, ≥ 1.5 ; $P < 0.05$; Online Figure VA). Among these differentially expressed genes, 15 showed binding sites for miR-320 in their promoter regions (sequences 2 kb upstream from the transcription start site), which we selected for further study (Online Figure VB). Of these, the expression of CD36 (an FA translocase) and VLDLR (very-low-density lipoprotein receptor) was significantly upregulated in rat H9c2, murine HL-1, human AC16, human primary cardiomyocytes, and NRVCs treated with miR-320 mimic (Figure 4B through 4D). CD36 and VLDLR expression was also increased in db/db mice upon rAAV-miR-320 treatment—an effect that was abrogated by rAAV-miR-320-TuD (Figure 4E and 4F; Online Figure VC).

To establish the functional connection between miR-320 and its candidate target genes, we treated isolated cardiomyocytes with miR-320 mimic or siRNAs against CD36 and VLDLR (si-CD36 and si-VLDLR). miR-320 or si-CD36/VLDLR was efficiently transfected into cardiomyocytes, while no effect on cardiomyocyte apoptosis was observed under normal physiological conditions (Online Figure VIA and VIB). However, when high glucose (33.3 mmol/L) and palmitate (0.5 mmol/L) were used to induce a diabetic state, we detected increased apoptosis with the miR-320 mimic, which could be reversed by the miR-320 inhibitor (Online Figure VIB). Importantly, miR-320-induced apoptosis and FFA uptake in cardiomyocytes could be completely or partly blocked by knocking down CD36 or VLDLR (Figure 5A and 5B; Online Figure VIC). When miR-320 was inhibited, overexpression of CD36 or VLDLR gave rise to similar results (Online Figure VID through VIF). These data point to the possibility that CD36 and VLDLR may be key downstream effectors of miR-320 in cardiomyocytes under diabetes mellitus conditions.

The stronger effect of CD36 indicated that the effects conferred by miR-320 were attributed mainly to the induced expression of this gene. We, therefore, selected *CD36* for further functional and mechanistic studies. We used db/db mice and cardiomyocyte-specific troponin T (tnt) vectors (rAAV-tnt; Online Figure VIG) to evaluate whether miR-320 aggravated DCM by modulating *CD36* expression in vivo. Sixteen weeks after treatment with rAAV-tnt-miR-320, we detected both increased miR-320 (Online Figure VIH through VIJ) and CD36 protein (Figure 5C) in the heart of db/db mice. While rAAV-tnt-miR-320 and rAAV-tnt-CD36 treatments had no effect on blood glucose levels (Online Figure VIK and VIL), such treatments clearly exacerbated cardiac dysfunction in db/db mice (Figure 5D). Inhibition of miR-320 with rAAV-miR-320-TuD and shRNA-mediated knockdown of CD36 with the rAAV-tnt-shRNA-CD36 vector abrogated this effect. Moreover, CD36 knockdown blocked rAAV-tnt-miR-320-induced cardiac dysfunction. In contrast, the protective effect of miR-320 inhibition with rAAV-miR-320-TuD was attenuated upon CD36 overexpression

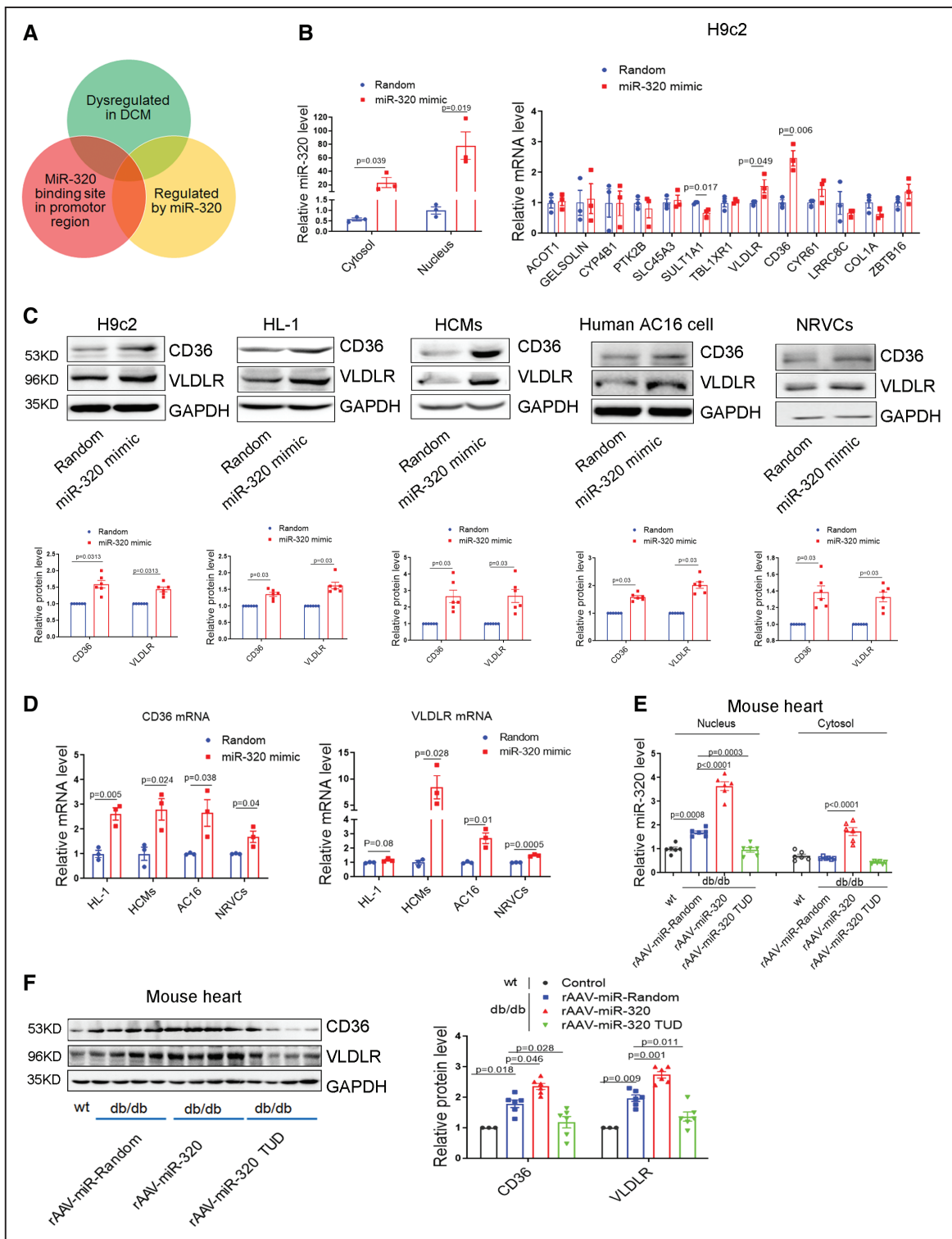


Figure 4. Nuclear miR-320 increases CD36 (fatty acid translocase) and VLDLR (very-low-density lipoprotein receptor) expression.

A, Strategy to identify nuclear targets for miR-320 in diabetic cardiomyopathy. **B**, Quantitative reverse transcription polymerase chain reaction (qRT-PCR) analysis of miR-320 regulation on target genes in H9c2 cardiomyocytes. **C**, Western blotting analysis of CD36 and VLDLR protein levels in rat H9c2, in murine HL-1, in human primary cardiomyocytes (HCMs), in human AC16 cell line, and in neonatal rat ventricular cardiomyocytes (NRVCs) transfected with miR-320 mimic. **D**, qRT-PCR analysis of CD36 and VLDLR mRNA levels in various cardiomyocytes transfected with miR-320 mimic. **E**, qRT-PCR analysis of nuclear and cytosol miR-320 levels in rAAV-miR-320-treated db/db mice. **F**, Western blotting analysis of CD36 and VLDLR protein levels in rAAV-miR-320-treated db/db mice. **B**, $n=3$; **(C)** $n=6$; **(D)** $n=3$; **(E and F)** $n=6$. **B and D**, Student t test; **(C)** Wilcoxon signed-rank test; **(E and F)** 1-way ANOVA followed by Bonferroni post test (number of comparisons, 6). Adjusted P values were provided in case of multiple groups. DCM indicates diabetic cardiomyopathy; and rAAV, recombinant adeno-associated virus.

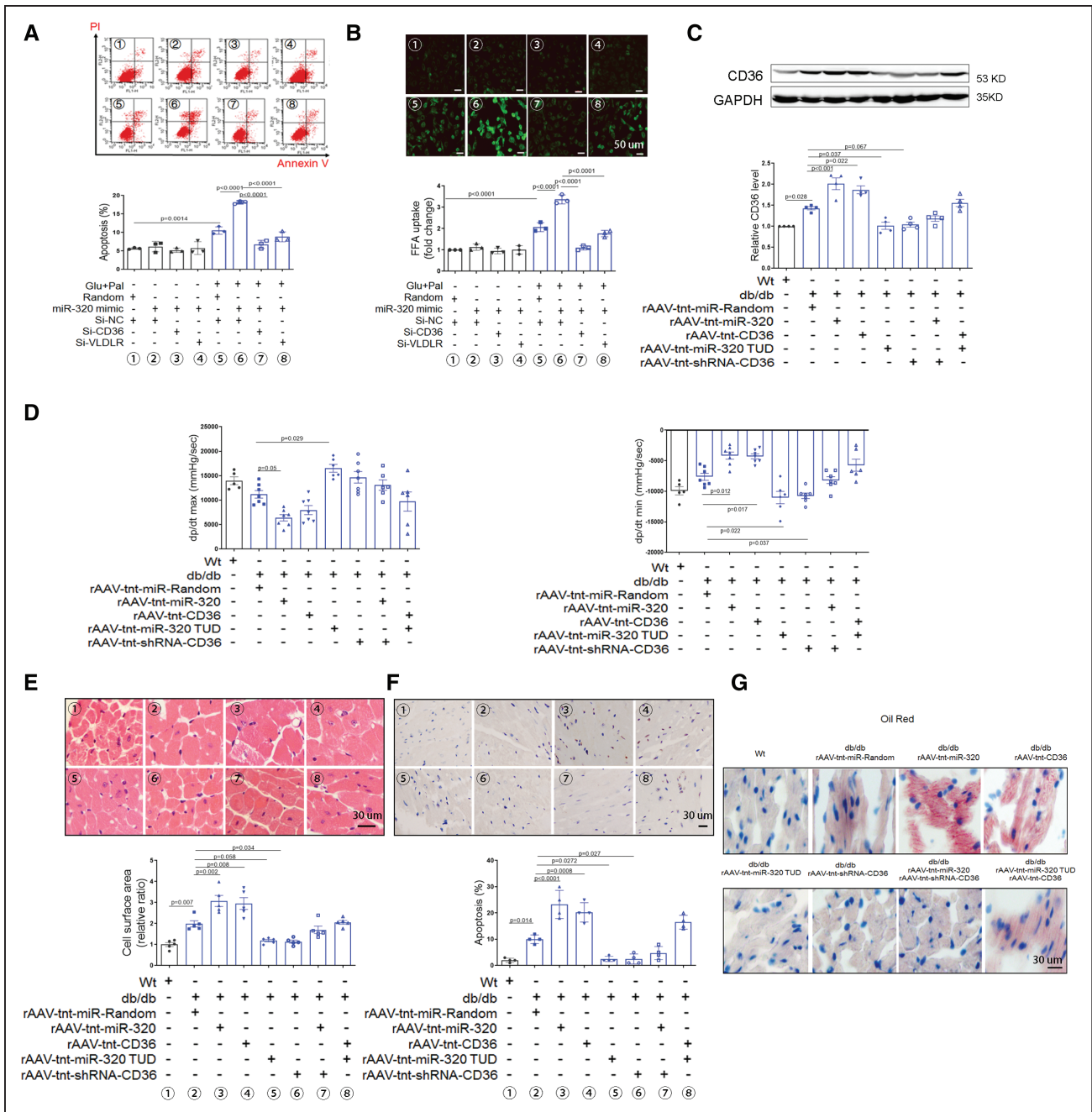


Figure 5. MiR-320 function in diabetes mellitus-induced cardiac dysfunction is mediated by CD36 (fatty acid translocase).

A, MiR-320-induced apoptosis was rescued by si-CD36 and si-VLDLR. **B**, Free fatty acid uptake stimulated by miR-320 was abolished by si-CD36 and si-VLDLR, as determined with the BODIPY FL C16 probe. **C–G**, CD36 levels (**C**); hemodynamic analysis (**D**); cardiomyocyte visualization and size (**E**); apoptosis (**F**); cardiac lipid deposition detected by Oil Red (**G**) in various groups. Glu, 33.3 mmol/L; Pal, 0.5 mmol/L for 24 h. **A** and **B**, n=3; (**C**) n=4; (**D**) n=5 to 8; (**E**) n=5; (**F** and **G**) n=4; (**A–F**) 1-way ANOVA followed by Bonferroni post test (number of comparisons, 28). rAAV indicates recombinant adeno-associated virus; and VLDLR, very-low-density lipoprotein receptor.

through rAAV-tnt-CD36 transduction (Figure 5D; Online Table IX). Consistently, we observed coordinated changes in myocardial tissue sections, heart fat deposition, reactive oxygen species levels, and apoptosis under different treatment conditions (Figure 5E through 5G; Online Figure VIM). Additionally, we also explored short-term effects (8 weeks) of rAAV-tnt-miR-320 treatment on cardiac function (Online Figure VIN). Notably, compared

with long-term interventions, the echocardiographic and hemodynamic data from short-term studies showed similar trends in db/db mice (Online Figure VIO through VIR; Online Table X), suggesting the consistent and lasting effects of miR-320/CD36 in DCM.

We further performed transcriptome analysis of isolated heart tissues from rAAV-tnt-miR-320-TuD-treated db/db mice, confirming decreased *CD36* transcription upon

miR-320 inhibition relative to control mice (Online Figure VIS; [Online Data Supplement](#)). This analysis further revealed that the miR-320-regulated transcriptome was highly related to diabetic cardiac dysfunction-related pathways according to Kyoto Encyclopedia of Genes and Genomes pathway analysis (Online Figure VIT). Collectively, these data demonstrated that miR-320 overexpression exacerbated DCM in diabetes mellitus mice and the advent effects could be rescued by suppressing either miR-320 or CD36.

Nuclear miR-320 Directly Activates CD36 Transcription

The mouse *CD36* promoter contains 7 putative miR-320-binding sites (Figure 6A). By chromatin immunoprecipitation sequencing, we found that Ago2 interacted with site 4 in HL-1 cells overexpressing miR-320 (Figure 6B; Online Figure VIIA through VIID). We further confirmed this result with chromatin immunoprecipitation qPCR and obtained similar results on rat H9c2 cardiomyocytes, human primary cardiomyocytes, and NRVCs (Online Figure VIIE through VIII). These data suggest that miR-320 directly targets the miRNA machinery to the *CD36* promoter.

To investigate the functional significance of miR-320-regulated expression of CD36, we constructed a pGL3 plasmid harboring the *CD36* promoter. miR-320 overexpression enhanced the fluorescence signal of pGL3-CD36 but not its mutated form (mutation A at site 4; Figure 6C). The sequence of site 4 was conserved between mice and humans (Online Figure VIJ). Consistent with the function of miR-320 at the level of transcription, siRNA-mediated knockdown of Ago2 prevented miR-320-induced upregulation of CD36 in cardiomyocytes (Figure 6D). Furthermore, we attempted to functionally rescue miR-320-enhanced *CD36* transcription in Ago2-depleted cardiomyocytes with an Ago2 fused to a nuclear localization signal. Interestingly, reexpression of nuclear Ago2 restored miR-320-dependant *CD36* transcription in adult human AC16 cardiomyocytes, as well as in primary NRVCs (Figure 6E and 6F; Online Figure VIIK). In contrast, we also engineered a cytosolic form of Ago2 by fusing it to a nuclear export signal and found that this cytosolic Ago2 was not able to rescue *CD36* transcription in Ago2 knockdown cells (Online Figure VIIL). These data provide strong evidence that nuclear miR-320/Ago2 is responsible for *CD36* activation in cardiomyocytes. A previous experiment showed that a designer small RNA that targets gene promoter is able to enhance the recruitment of RNA Pol II to activate gene expression.¹⁷ In line with this observation, we also detected an increased association of Ago2 with RNA polymerase II in cardiomyocytes treated with miR-320 mimic (Figure 6G). Corroborating with elevated *CD36* transcription, we verified elevated RNA Pol II occupancy by chromatin immunoprecipitation qPCR on the *CD36* promoter in rat

H9c2, murine HL-1, rat NRVCs, and human primary cardiomyocytes treated with miR-320 mimic (Online Figure VIIM). In db/db mice, increased association of Ago2 and RNA polymerase II with *CD36* promoter were abrogated by rAAV-tnt-miR-320-TuD treatment (Online Figure VIIN and VIIO). We showed that miR-320 mimic had no effect on the stability of *CD36* mRNA (Online Figure VIIP). Together, these data suggest that miR-320 directly activates *CD36* transcription in the nucleus.

DISCUSSION

Our results demonstrated that miR-320 is upregulated in the heart by hyperglycemia, which acts in the nucleus to enhance *CD36* transcription. As CD36 is known to promote FA uptake and myocardial lipid deposition, this raises a possibility that gluco- and lipotoxicity might mutually enforce one another, thus collectively contributing to diabetes mellitus-induced cardiac dysfunction (Online Figure VIIQ and VIIR). Importantly, we showed that miR-320 inhibition is able to effectively rescue cardiac dysfunction in diabetic mice.

Interestingly, miR-320 was increased in cardiomyocytes but remained unchanged in noncardiomyocytes. This has been preceded with other miRNAs. For example, miR-132 was elevated in myocytes but decreased in cardiac fibroblast in pressure overloading-induced heart failure mice.¹⁸ Conversely, miR-21 was reported to show increased expression in fibroblasts but remained unchanged in myocytes during heart failure.¹⁹ Thus, the same miRNA may function in different cell types. Indeed, miR-21 overexpression in fibroblast has been shown to promote cardiac fibrosis but protect against cardiac hypertrophy in myocytes.^{8,19,20} Our current findings suggest that miR-320 is another cell type-specific regulator. Further studies will investigate how other miRNAs might be differentially expressed in cardiomyocytes versus other cell types in the heart during development or disease processes.

The divided tasks of miRNAs in different cellular compartments are interesting regulatory paradigms. Most miRNAs are present in both the nucleus and the cytoplasm, with some showing selective nuclear enrichment.²¹ For example, miR-29b is mainly nuclear, whereas miR-29a is predominantly cytoplasmic in HeLa cells.²² The major difference between these 2 miRNAs is the presence of a hexanucleotide sequence (AGUGUU) at the 3' end of miR-29b, and insertion of this motif into an siRNA-targeting luciferase was found to be sufficient for nuclear targeting.²² Other miRNAs containing 3' UGUGUU, ACUGUU, AGAGUU, AGUCUU, AGUGAU, AGUGUA, and AGNGUN sequences are also known to accumulate in the nucleus.²³ We noted related GU-rich motifs in miR-320, but which of these motifs are responsible for nuclear targeting awaits further investigation.

It is currently unclear how exactly miR-320 activates transcription in the nucleus. The mechanism might be

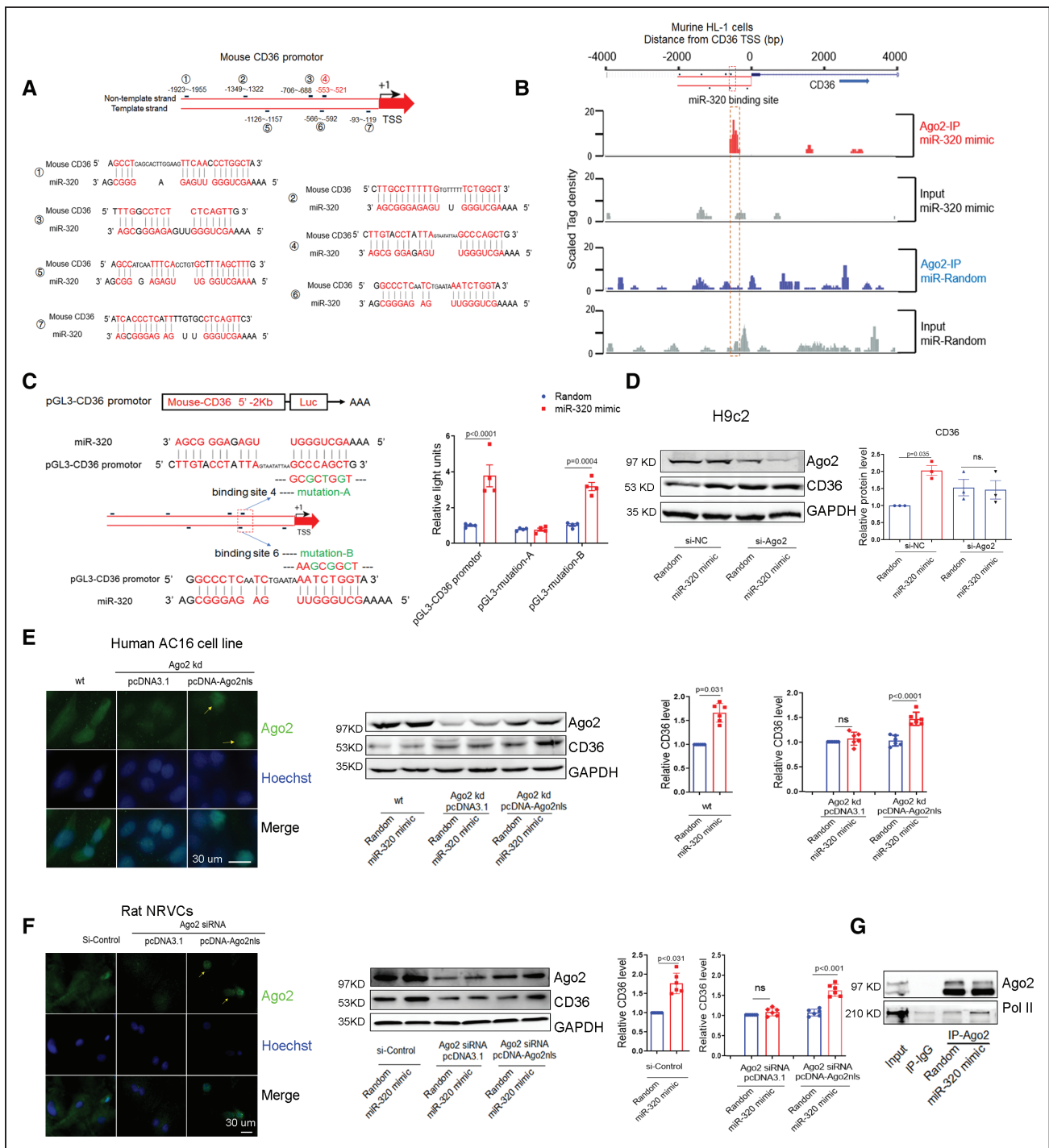


Figure 6. Nuclear miR-320 activates *CD36* (fatty acid translocase) transcription.

A, Sequence alignment of miR-320-binding sites in the promoter of mouse *CD36*. **B**, Ago2 (argonaute RISC catalytic component 2) chromatin immunoprecipitation sequencing profiles of input DNA and immunoprecipitation (IP) in murine HL-1 cardiomyocytes transfected with miR-320 mimic or random. Input samples are shown on the same scale as immunoprecipitates. **C**, Wild-type and mutated *CD36* promoter activities were determined with the luciferase reporter assays in HEK293 (human embryonic kidney 293) cells in response to miR-320 mimic treatment. **D**, Effects of miR-320 on *CD36* protein expression was abolished in the absence of Ago2. **E** and **F**, Western blotting analysis of the effects of miR-320 on *CD36* rescued with nuclear Ago2 reexpression (kd) AC16 cells (**E**) and neonatal rat ventricular cardiomyocytes (NRVCs; **F**). **G**, H9c2 cells were treated with miR-320 mimic and subsequently subjected to immunoprecipitation with an anti-Ago2 antibody to evaluate its interaction with RNA polymerase II. **C**, $n=4$; (**D**) $n=3$; (**E** and **F**) $n=6$; (**G**) $n=3$; (**C** and **D**) 1-way ANOVA followed by Bonferroni post test; (**E** and **F**) Wilcoxon signed-rank test and 1-way ANOVA followed by Bonferroni post test (**C**: number of comparisons, 15; **D**–**F**: number of comparisons, 6). Adjusted P values were provided in case of multiple groups. TSS indicates transcription start site.

related to a phenomenon known as small activating RNAs. It has been previously shown that such designer small activating RNA is able to target Ago2 to specific gene promoters through inducing the assembly of an RNA-induced transcription activation complex, which also contains components of the PAF1 (polymerase-associated factor 1) complex.²⁴ We suspect that miR-320 might activate transcription in a similar manner, and if so, our study would provide an *in vivo* example for a natural small activating RNA to activate transcription and link such regulation to an important disease process.

Diabetes mellitus-induced cardiac dysfunction is characterized by diastolic dysfunction at early stage, which has been linked to myocardial fibrosis, increased cardiac lipid accumulation, and altered calcium homeostasis.² We did not observe myocardial fibrosis in HFD-induced diabetes mellitus or db/db mice, consistent with previous studies.²⁵ Myocardial steatosis (lipid accumulation) is another independent predictor of diastolic dysfunction in type 2 diabetes mellitus.²⁶ We observed increased cardiac lipid accumulation in diabetic mice, which is further enhanced by miR-320, suggesting that miR-320 may exacerbate diastolic dysfunction of DCM by promoting cardiac lipid accumulation.

Metabolic disturbance is aggravated in miR-320 tg mice when combined with HFD-induced diabetes mellitus. We previously showed that miR-320 overexpression increased plasma levels of cholesterol and triglycerides in ApoE-null mice.²⁷ In the present study, we found that cardiac-specific overexpression of miR-320 exacerbated cardiac dysfunction in db/db mice, and conversely, neutralizing miR-320 with rAAV-tnt-miR-320-TuD effectively reversed the phenotype of diabetes mellitus-induced cardiac dysfunction, suggesting a potential therapeutic strategy for the treatment of diabetes mellitus-triggered cardiac dysfunction. In terms of diabetes mellitus itself, because cardiac miR-320 overexpression did not affect blood glucose levels (Online Figure VIK and VII), the contribution of miR-320 to diabetes mellitus is likely through noncardiac tissues. Indeed, our unpublished results showed that liver- or fat-specific overexpression of miR-320 both increased glucose level and enhanced insulin resistance in db/db mice. In fact, diabetes mellitus is well known multiple-tissue disorders, including liver, adipose, pancreas, skeletal muscle and brain, which are far more complicated than just DCM. Therefore, miR-320 might have distinct or even opposite roles in these tissues, which needs further investigation.

Interestingly, cardiac miR-320 overexpression was sufficient to induce CD36 expression under both normal and diabetic conditions but only exacerbated cardiac function under diabetic condition. In fact, CD36 itself—the direct target of nuclear miR-320—showed a similar effect as miR-320 that CD36 only exacerbated cardiac function in db/db mice but not in normal mice, which was in line with a previous study showing that cardiac CD36 overexpression using AAV9 (adeno-associated virus serotype

9) alone was unable to induce cardiac physiological or morphological changes in normal mice.²⁸ Moreover, we found that CD36 overexpression in cultured cardiomyocytes enhanced apoptosis only in the presence of FFA and high glucose (Online Figure VIB). This is also the case in murine kidney collecting duct cells where overexpressed CD36 alone was found to be insufficient to trigger apoptosis.²⁹ It appears that excessive CD36 and miR-320 are able to enhance apoptosis and cardiac dysfunction only in the presence of initial stresses, such as FFA and high glucose (Online Figure VIQ). This might explain why under physiological conditions, overexpression of CD36 or miR-320 alone appears to be insufficient to induce damages in cultured cells or normal hearts.

Nonesterified FA level and hyperglycemia are known triggers for the cardiac phenotype in diabetes mellitus. CD36 is involved in nonesterified FA uptake into intestinal enterocytes, adipocytes, and skeletal and cardiac myocytes.²⁹ Our findings suggest a critical role of CD36 in FA transport in the heart, which is consistent with the observation that loss of CD36 could rescue myocardial neutral lipid imbalance and cardiac dysfunction in a mouse model of DCM.³⁰ Our data suggest that CD36 is an indispensable component of the FA cellular transport system in the heart, consistent with a dominant role of CD36 over other proteins implicated in FFA transport.³⁰ However, we also noted another FFA transporter, FA-binding protein 3, as a target for miR-320 (Online Figure VIS), suggesting that miR-320 may modulate multiple related components in the pathway (Online Figure VIT), which may collectively contribute to diabetes mellitus-induced cardiac dysfunction progression. Besides lipid uptake, miR-320 and CD36 (but not VLDLR) also increased lipotoxic catabolite diacylglycerol and reactive oxygen species levels and decreased mitochondrial ETC (electron transport chain) gene expression and ATP production (Online Figure VIIS). These mechanisms might thus collectively contribute to miR-320-induced lipotoxicity and explain why apoptosis could be completely blocked by knocking down CD36 but only partly blocked by knocking down VLDLR.

In terms of FA oxidation (FAO), we noted that FAO rates (determined by O₂ consumption) were unaffected by miR-320 or CD36 overexpression (Online Figure VIU). This is actually consistent with a previous study demonstrating that kidney-specific overexpression of CD36 led to considerable accumulation of intracellular lipids, while the quantitative analysis of FAO markers indicated almost no change in CD36-tg kidney. Another study using CD36 overexpressed primary mouse hepatocytes also suggested that lipid increase was directly related to CD36-mediated FA uptake as opposed to its role in channeling FAs to oxidation.^{31,32} Notably, there are also several studies implicating a role of CD36 in promoting FAO. For example, CD36 ablated heart showed decreased FAO in young mice but no effect on aged mice.³³ In myotubes, CD36 knockdown decreased FAO; however, CD36 knockdown increased

FAO when myotubes were permeabilized with digitonin to bypass CD36-mediated FA uptake.³⁴ Another study showed that the effects of CD36 on FAO in muscle cells differed at different concentrations of FFA pretreated.³⁵ These results suggest a possibility that CD36 may play a predominant role in FFA uptake, which may indirectly affect FAO. Therefore, our data only suggested that in this particular pathophysiological state, miR-320 and CD36 increased lipid accumulation (Online Figure VIIT) was likely through activated FA uptake rather than changed FAO (Online Figure VIU). However, considering the dynamic regulation of FFA on FAO, whether miR-320 or CD36 affected FAO in a shorter/longer time window or another disease model remained to be determined in the future.

Importantly, our data show that the miR-320/CD36 pathway induces both gluco- and lipotoxicity. Metabolic disturbances in the diabetic state include hyperlipidemia and early hyperinsulinemia followed by pancreatic β -cell failure, which eventually leads to hyperglycemia.⁴ In our HFD-induced diabetic model, we found that miR-320 is upregulated in the heart after the onset of hyperglycemia, which increases CD36 expression and lipid uptake by cardiomyocytes, thus perpetuating a negative cycle of lipotoxicity and cardiac dysfunction under diabetes mellitus conditions (Online Figure VIIR).

Strikingly, we found that exogenous miR-320 TuD (inhibitor) delivered by rAAV was sufficient to rescue cardiac dysfunction in various diabetic models. We noted a previous report by Hideo Iba, suggesting the ability of miRNA-TuD to be directly target to the nucleus.³⁶ We found that although exogenous miR-320 TuD was detectable both in the nucleus and the cytoplasm, TuD transfection appears to be more effective in reducing nuclear miR-320 (Online Figure VIIV). Such selective effect might result from TuD action in the nucleus to reduce nuclear miR-320 or from TuD-mediated sequestration of miR-320 in the cytoplasm, thereby preventing the translocation of miR-320 into the nucleus, possibilities to be differentiated in future studies. Importantly, our data provided concrete evidence that TuD-based miR-320 inhibition was sufficient to reduce nuclear miR-320 and rescue cardiac dysfunction in diabetic mice.

In summary, our findings reveal a novel function of miR-320 as a positive regulator of gene transcription and demonstrate that miR-320 inhibition can rescue DCM in diabetic mice. These findings suggest a potential therapeutic strategy for the treatment of diabetes mellitus-induced cardiac dysfunction by targeting miR-320.

ARTICLE INFORMATION

Received February 11, 2019; revision received October 11, 2019; accepted October 18, 2019.

Affiliations

From the Division of Cardiology, Department of Internal Medicine, Tongji Hospital, Tongji Medical College, Huazhong University of Science and Technology, Wuhan, China (H.L., J.F., Y.Z., B.D., J.Z., X.N., C.C., D.W.W.); Hubei Key Laboratory of Genetics and Molecular Mechanisms of Cardiologic Disorders, Wuhan, China

(H.L., J.F., Y.Z., B.D., J.Z., X.N., C.C., D.W.W.); Key Laboratory of RNA Biology, Institute of Biophysics, Chinese Academy of Sciences, Beijing (X.Z.); and Department of Cellular and Molecular Medicine, Institute of Genomic Medicine, University of California, La Jolla, San Diego (X.-D.F.).

Acknowledgments

We thank our colleagues in Dr Wang's group for technical assistance and stimulating discussions during the course of this investigation.

Sources of Funding

This work was supported by grants from the National Natural Science Foundation of China (No. 81822002, 91439203, 91839302, 81630010, 31771264, 81790624, and 31800973) and the Fundamental Research Funds for the Central Universities (2019kfyXMBZ035). The funders had no role in study design, data collection and analysis, manuscript preparation, or decision to publish.

Disclosures

None.

REFERENCES

- Haffner SM, Lehto S, Rönnemaa T, Pyörälä K, Laakso M. Mortality from coronary heart disease in subjects with type 2 diabetes and in nondiabetic subjects with and without prior myocardial infarction. *N Engl J Med*. 1998;339:229–234. doi: 10.1056/NEJM199807233390404
- Boudina S, Abel ED. Diabetic cardiomyopathy, causes and effects. *Rev Endocr Metab Disord*. 2010;11:31–39. doi: 10.1007/s11154-010-9131-7
- Gilbert RE, Krum H. Heart failure in diabetes: effects of anti-hyperglycaemic drug therapy. *Lancet*. 2015;385:2107–2117. doi: 10.1016/S0140-6736(14)61402-1
- Poornima IG, Parikh P, Shannon RP. Diabetic cardiomyopathy: the search for a unifying hypothesis. *Circ Res*. 2006;98:596–605. doi: 10.1161/01.RES.0000207406.94146.c2
- Winhofer Y, Krssák M, Jankovic D, Anderwald CH, Reiter G, Hofer A, Trattig S, Luger A, Krebs M. Short-term hyperinsulinemia and hyperglycemia increase myocardial lipid content in normal subjects. *Diabetes*. 2012;61:1210–1216. doi: 10.2337/db11-1275
- Packer M. Reconceptualization of the molecular mechanism by which sodium-glucose cotransporter 2 inhibitors reduce the risk of heart failure events. *Circulation*. 2019;140:443–445. doi: 10.1161/CIRCULATIONAHA.119.040909
- Costantino S, Paneni F, Lüscher TF, Cosentino F. MicroRNA profiling unveils hyperglycaemic memory in the diabetic heart. *Eur Heart J*. 2016;37:572–576. doi: 10.1093/eurheartj/ehv599
- Li H, Zhang X, Wang F, Zhou L, Yin Z, Fan J, Nie X, Wang P, Fu XD, Chen C, et al. MicroRNA-21 lowers blood pressure in spontaneous hypertensive rats by upregulating mitochondrial translation. *Circulation*. 2016;134:734–751. doi: 10.1161/CIRCULATIONAHA.116.023926
- Moshkovich N, Nisha P, Boyle PJ, Thompson BA, Dale RK, Lei EP. RNAi-independent role for Argonaute2 in CTCF/CP190 chromatin insulator function. *Genes Dev*. 2011;25:1686–1701. doi: 10.1101/gad.16651211
- Yang S, Chen C, Wang H, Rao X, Wang F, Duan Q, Chen F, Long G, Gong W, Zou MH, et al. Protective effects of Acyl-coA thioesterase 1 on diabetic heart via PPAR α /PGC1 α signaling. *PLoS One*. 2012;7:e50376. doi: 10.1371/journal.pone.0050376
- Duong Van Huyen JP, Tible M, Gay A, Guillemain R, Aubert O, Varnous S, Iserin F, Rouvier P, François A, Vernerey D, et al. MicroRNAs as non-invasive biomarkers of heart transplant rejection. *Eur Heart J*. 2014;35:3194–3202. doi: 10.1093/eurheartj/ehu346
- Yu D, Tolleson WH, Knox B, Jin Y, Guo L, Guo Y, Kadlubar SA, Ning B. Modulation of ALDH5A1 and SLC22A7 by microRNA hsa-miR-29a-3p in human liver cells. *Biochem Pharmacol*. 2015;98:671–680. doi: 10.1016/j.bcp.2015.09.020
- Hummel KP, Dickie MM, Coleman DL. Diabetes, a new mutation in the mouse. *Science*. 1966;153:1127–1128. doi: 10.1126/science.153.3740.1127
- Qi Y, Xu Z, Zhu Q, Thomas C, Kumar R, Feng H, Dostal DE, White MF, Baker KM, Guo S. Myocardial loss of IRS1 and IRS2 causes heart failure and is controlled by p38 α MAPK during insulin resistance. *Diabetes*. 2013;62:3887–3900. doi: 10.2337/db13-0095
- Li HP, Fan JH, Yin ZW, Wang F, Chen C, Wang DW. Identification of cardiac-related circulating microRNA profile in human chronic heart failure. *Oncotarget*. 2016;7:33–45
- Inagaki K, Fuess S, Storm TA, Gibson GA, Mctiernan CF, Kay MA, Nakai H. Robust systemic transduction with AAV9 vectors in mice: efficient global

- cardiac gene transfer superior to that of AAV8. *Mol Ther*. 2006;14:45–53. doi: 10.1016/j.yjthe.2006.03.014
17. Schwartz JC, Younger ST, Nguyen NB, Hardy DB, Monia BP, Corey DR, Janowski BA. Antisense transcripts are targets for activating small RNAs. *Nat Struct Mol Biol*. 2008;15:842–848. doi: 10.1038/nsmb.1444
 18. Ucar A, Gupta SK, Fiedler J, Erikci E, Kardasinski M, Batkai S, Dangwal S, Kumarswamy R, Bang C, Holzmann A, et al. The miRNA-212/132 family regulates both cardiac hypertrophy and cardiomyocyte autophagy. *Nat Commun*. 2012;3:1078. doi: 10.1038/ncomms2090
 19. Thum T, Gross C, Fiedler J, Fischer T, Kissler S, Bussen M, Galuppo P, Just S, Rottbauer W, Frantz S, et al. MicroRNA-21 contributes to myocardial disease by stimulating MAP kinase signalling in fibroblasts. *Nature*. 2008;456:980–984. doi: 10.1038/nature07511
 20. Ramanujam D, Sassi Y, Laggenbauer B, Engelhardt S. Viral vector-based targeting of miR-21 in cardiac nonmyocyte cells reduces pathologic remodeling of the heart. *Mol Ther*. 2016;24:1939–1948. doi: 10.1038/mt.2016.166
 21. Khudayberdiev SA, Zampa F, Rajman M, Schrott G. A comprehensive characterization of the nuclear microRNA repertoire of post-mitotic neurons. *Front Mol Neurosci*. 2013;6:43. doi: 10.3389/fnmol.2013.00043
 22. Hwang HW, Wentzel EA, Mendell JT. A hexanucleotide element directs microRNA nuclear import. *Science*. 2007;315:97–100. doi: 10.1126/science.1136235
 23. Mendell JT, Hwang HW, Wentzel EA. Nucleotide motifs providing localization elements and methods of use. World Intellectual Property Organization. 2007; WO 2007/149521 A2.
 24. Portnoy V, Lin SH, Li KH, Burlingame A, Hu ZH, Li H, Li LC. saRNA-guided Ago2 targets the RITA complex to promoters to stimulate transcription. *Cell Res*. 2016;26:320–335. doi: 10.1038/cr.2016.22
 25. Van den Bergh A, Vanderper A, Vangheluwe P, Desjardins F, Nevelsteen I, Verreth W, Wuytack F, Holvoet P, Flameng W, Balligand JL, et al. Dyslipidaemia in type II diabetic mice does not aggravate contractile impairment but increases ventricular stiffness. *Cardiovasc Res*. 2008;77:371–379. doi: 10.1093/cvr/cvm001
 26. Rijzewijk LJ, van der Meer RW, Smit JW, Diamant M, Bax JJ, Hammer S, Romijn JA, de Roos A, Lamb HJ. Myocardial steatosis is an independent predictor of diastolic dysfunction in type 2 diabetes mellitus. *J Am Coll Cardiol*. 2008;52:1793–1799. doi: 10.1016/j.jacc.2008.07.062
 27. Chen C, Wang Y, Yang S, Li H, Zhao G, Wang F, Yang L, Wang DW. MiR-320a contributes to atherogenesis by augmenting multiple risk factors and down-regulating SRF. *J Cell Mol Med*. 2015;19:970–985. doi: 10.1111/jcmm.12483
 28. Guo Y, Wang Z, Qin X, Xu J, Hou Z, Yang H, Mao X, Xing W, Li X, Zhang X, et al. Enhancing fatty acid utilization ameliorates mitochondrial fragmentation and cardiac dysfunction via rebalancing optic atrophy 1 processing in the failing heart. *Cardiovasc Res*. 2018;114:979–991. doi: 10.1093/cvr/cvy052
 29. Susztak K, Ciccone E, McCue P, Sharma K, Böttinger EP. Multiple metabolic hits converge on CD36 as novel mediator of tubular epithelial apoptosis in diabetic nephropathy. *PLoS Med*. 2005;2:e45. doi: 10.1371/journal.pmed.0020045
 30. Yang J, Sambandam N, Han X, Gross RW, Courtois M, Kovacs A, Febbraio M, Finck BN, Kelly DP. CD36 deficiency rescues lipotoxic cardiomyopathy. *Circ Res*. 2007;100:1208–1217. doi: 10.1161/01.RES.0000264104.25265.b6
 31. Kang HM, Ahn SH, Choi P, Ko YA, Han SH, Chinga F, Park AS, Tao J, Sharma K, Pullman J, et al. Defective fatty acid oxidation in renal tubular epithelial cells has a key role in kidney fibrosis development. *Nat Med*. 2015;21:37–46. doi: 10.1038/nm.3762
 32. Koonen DP, Jacobs RL, Febbraio M, Young ME, Soltys CL, Ong H, Vance DE, Dyck JR. Increased hepatic CD36 expression contributes to dyslipidemia associated with diet-induced obesity. *Diabetes*. 2007;56:2863–2871. doi: 10.2337/db07-0907
 33. Koonen DP, Febbraio M, Bonnet S, Nagendran J, Young ME, Michalakis ED, Dyck JR. CD36 expression contributes to age-induced cardiomyopathy in mice. *Circulation*. 2007;116:2139–2147. doi: 10.1161/CIRCULATIONAHA.107.712901
 34. Samovski D, Sun J, Pietka T, Gross RW, Eckel RH, Su X, Stahl PD, Abumrad NA. Regulation of AMPK activation by CD36 links fatty acid uptake to β -oxidation. *Diabetes*. 2015;64:353–359. doi: 10.2337/db14-0582
 35. García-Martínez C, Marotta M, Moore-Carrasco R, Guitart M, Camps M, Busquets S, Montell E, Gómez-Foix AM. Impact on fatty acid metabolism and differential localization of FATP1 and FAT/CD36 proteins delivered in cultured human muscle cells. *Am J Physiol Cell Physiol*. 2005;288:C1264–C1272. doi: 10.1152/ajpcell.00271.2004
 36. Haraguchi T, Ozaki Y, Iba H. Vectors expressing efficient RNA decoys achieve the long-term suppression of specific microRNA activity in mammalian cells. *Nucleic Acids Res*. 2009;37:e43. doi: 10.1093/nar/gkp040